The south-verging Isortoq Nappe of Baffin Island, Canada: implications on the framework of the NE Trans-Hudson Orogen

Benoit M. Saumur Département des Sciences de la Terre et de l'atmosphère, Université du Québec à Montréal, 201 av. du Président-Kennedy, Montréal, QC, H2X 3Y7, saumur.benoit-michel@uqam.ca; *TWITTER :* @saumurbe

Stephen T. Johnston Department of Earth and Atmospheric Science, University of Alberta, Edmonton, AB, T6G 2E3

Diane R. Skipton Yukon Geological Survey, 918 Alaska Highway, Whitehorse, YU, Y1A 6E7

&

Marc St-Onge Geological Survey of Canada, Central Canada Division, 601 Booth St., Ottawa, ON., K1A 0E8

Submitted for peer review to *Canadian Journal of Earth Sciences*

February 20 2022

The south-verging Isortoq Nappe of Baffin Island, Canada: implications on the framework of the NE Trans-Hudson Orogen

Saumur, B.M., Johnston, S.T., Skipton, D.R. and St-Onge, M.R.

Abstract

The Isortoq Shear Zone (ISZ), a 100km-scale structure in northern Baffin Island, was identified in the 1970s through the interpretation of regional geophysical surveys. However, the ISZ is cryptic in the field, and its origin and significance with respect to the regional structural framework of northern Baffin Island remained ambiguous. Recent mapping along the ISZ, as well as within the Archean Isortoq and Eqe Bay greenstone belts of central-west Baffin Island, provides new regional structural constraints. We show that the Isortoq and Eqe Bay belts form one continuous folded supracrustal package that was likely deformed by nappe tectonics during the early Paleoproterozoic Trans-Hudson Orogeny. The northern NE-striking, moderately SE-dipping Isortoq belt is structurally thinned, metamorphosed, sheared (by the ISZ) and overturned, with strata younging down-section to the NW. In contrast, the southern ENE-striking, steeply dipping Eqe Bay belt is structurally thickened, comparatively less metamorphosed, exhibits weaker deformation, and stratigraphically youngs to the SE. New mapping and available geophysical data show that the two belts are folded around a hinge zone located offshore to the SW, within nearby Grant-Suttie Bay, and together form an asymmetric synformal anticline. Structural and stratigraphic relationships are consistent with the fold forming part of the lower limb of a map-scale southeast-verging nappe, with the ISZ representing a shear zone at the base of this nappe. The Isortoq Nappe occurs along

strike with SW-verging Rinkian nappes exposed >200 km to the NE, on Baffin Island and in Greenland. This implies that south-verging tectonics, opposed to and predating the dominant N-verging nappes of the Foxe Fold Belt, are more important in spatial extent than previously considered, and emphasises the importance of horizontal transport via nappe tectonics during the construction of the Nuna Supercontinent.

Keywords: Arctic Canada, Mary River Group, Piling Group, Rae Craton, structural geology, nappe tectonics

Introduction

Nappes are ubiquitous regional-scale structures within Phanerozoic orogens (e.g. McClay and Price 1981), and although they have also been documented in Proterozoic and Archean terranes (e.g. de Wit, 1982; Friend and Nutman 1991), their recognition in polydeformed and deeply eroded terranes is relatively difficult. Their identification depends upon the preservation of structural elements that are considered characteristic of nappes (e.g. Ramsay 1981; Bastida et al. 2014). These include (but are not limited to) synformal anticlines and antiformal synclines along the overturned lower limb of a nappe, as well as asymmetric, mesoscopic-scale, parasitic folds that verge in the opposite direction of nappe emplacement and are characterised by thinned upper and lower limbs that connect through a steeply-dipping and structurally thickened short limb. Linear elements include two perpendicular coeval lineations; a fold axis parallel intersection lineation, and a stretching lineation that records the transport / emplacement direction of the nappe.

The identification of regional-scale tectonic elements is further hindered in remote, frontier areas, such as large swaths of Canada's Arctic, which remain sparsely inhabited and are therefore difficult to access for traditional boots-on-the-ground fieldwork. Regional geophysical surveys and associated enhancement techniques and filters (e.g. Beauchemin et al. 2018), as well as modern remote predictive mapping by satellite imagery (e.g. He et al. 2015), provide first order constraints and are key for targeting areas of interest. Although these supplement the collection of structural field data, a recognition and comprehension of regional structures requires the collection of mesoscale structural data that provide quantitative 3D geometric and kinematic constraints.

The geology of remote northern Baffin Island (Nunavut, Canada) remains poorly understood despite recent regional-scale bedrock mapping campaigns (Skipton et al. 2017; Saumur et al. 2018; Steenkamp et al. 2018; Lebeau et al. 2019). Nevertheless, the area is key for our understanding of the kinematics of the Paleoproterozoic Trans-Hudson Orogen (THO) and regional tectonic correlations between Canada and Greenland (St-Onge et al. 2009, 2020). In addition, with the exception of the world-class Mary River Fe-deposit, greenstone belts of the Neoarchean Mary River Group have untapped mineral potential (Harrison et al. 2022). Among the least well-understood regional bedrock structural elements of northern Baffin Island is the Isortoq Shear Zone (ISZ; Jackson 2000; Jackson and Berman 2000), a regional-scale structural feature with a pronounced linear trace that has been well-constrained by airborne magnetics (Fig. 1). In this contribution, we report new structural observations and data stemming from geological mapping of the Grant-Suttie Bay area of northwestern Baffin Island. We provide a new interpretation for the ISZ, and argue that it, along with the two greenstone belts of the Grant-Suttie Bay area, forms part of a regional-scale synformal anticline developed along the lower, overturned limb of a south-verging tectonic nappe. These findings have implications for the regional architecture and the tectonic framework of northern Baffin Island and the northeastern THO as a whole, and highlight the importance of horizontal displacements during early Paleoproterozoic orogenesis.

Background

The geometry and kinematics of the Paleoproterozoic (ca. 1915-1758 Ma) THO, which formed as a result of the convergence and collision of the upper-plate Churchill domain with the lower-plate Superior Craton (Hoffman 1988; Lewry and Collerson 1990; St-Onge et al. 2006; Weller et al. 2021), are relatively well-defined on mainland Nunavut and central to southern Baffin Island (Fig. 1A). In comparison, the significance of THO structures in northern Baffin Island remains ambiguous. Reconnaissance-scale maps (e.g., Jackson et al. 1978; Jackson and Morgan 1978; Morgan 1982) describe the general geology of northern Baffin Island, and more recent 1:100,000-scale geological maps (Skipton et al. 2017; Saumur et al. 2018; Skipton et al. 2020a, b) provide geological constraints. The Churchill domain consists of several Archean-Paleoproterozoic crustal blocks, including the Archean Rae Craton of northern Canada and Greenland (St-Onge et al. 2006, 2009, 2020; Corrigan et al. 2009). Cratonic rocks of northern Baffin Island include Meso- to Neoarchean (ca. 2901-2706 Ma) orthogneiss and plutons, which range in composition from diorite to monzogranite, and subordinate greenstone belts of the ca. 2830-2705 Ma Mary River Group (Bethune and Scammell 1997; Skipton et al. 2017; 2019; Saumur et al. 2018). Unconformably overlying the Archean rocks are siliciclastic-carbonate strata and subordinate mafic-ultramafic volcanic rocks of the Paleoproterozoic Piling Group (e.g., Morgan et al. 1976; Henderson and Tippett 1980; Scott et al. 2002; Partin et al. 2014), which formed along the southeastern margin of the Archean Rae craton (e.g., Rainbird et al. 2010; Wodicka et al. 2014), and were subsequently deformed and metamorphosed during the THO (Gagné et al. 2009). Archean crust on northern Baffin Island is characterised by late Archean (ca. 3.0-2.5 Ga) deformation attributed to the Committee fold belt (Jackson and Taylor 1972), and is bound to the southeast by the north-verging Paleoproterozoic (ca. 1.88-1.865 Ma) Foxe Fold Belt (Fig. 1), which has been considered to represent the northern margin of the THO (e.g., St-Onge et al. 2009; Corrigan et al. 2009; Weller et al. 2021). The SW-verging ca. 1.88 Ga Rinkian fold belt (Fig. 1A) is identified both on NE Baffin Island (Jackson and Berman 2000) and in western Greenland (e.g., Kalsbeek 1986; Grocott and Pulvertaft 1990), and has been interpreted as the product of an early phase of THO deformation.

The southeast-dipping, east-northeast-striking ISZ consists of a narrow (10 to 100 metre wide) corridor of brittle-ductile fault rocks within Rae Craton granitoids and orthogneisses (e.g., Jackson 2000; Bethune and Scammell 2003b) that is coincident with a sharp break in regional aeromagnetic response (Fig. 1B; Natural Resources Canada 2020); a pronounced magnetic low southeast of the ISZ contrasts with magnetic highs to the northwest. The northeastern extension of this aeromagnetic signature is less clear: the zone is inferred by some to continue towards the northeastern coast of Baffin Island (see review by St-Onge et al. 2020), while others invoke the presence of a northeast Baffin thrust zone that truncates the aeromagnetic break ~50 km inland from the coast (Jackson et al. 1990). Regionally, the ISZ juxtaposes orthopyroxene-bearing felsic plutonic rocks and granulite facies assemblages to the northwest (Dexterity granulite belt) against lower grade, upper-amphibolite–facies rocks to the southeast (Jackson 2000; Saumur et al. 2018). The distribution of rocks that contain diagnostic granulite-facies assemblages northwest of the ISZ is, however, patchy and discontinuous (Skipton et al. 2020a,b). Previous interpretations of the ISZ include that it forms a regional suture zone marking the southern extent of the late Archean/Paleoproterozoic Committee Orogen (Jackson 2000) or that it is a northwest-verging thrust fault along which the Foxe Fold Belt and its basement have been placed over Archean crust of northern Baffin Island during the THO, at ca. 1850–1820 Ma (Jackson and Berman 2000; Bethune and Scammell 2003b).

The ISZ and the Isortoq belt

Two greenstone belts, the more northerly, SE-dipping Isortoq and the more southerly, sub-vertical, ENE-striking Eqe Bay belts, occur in the vicinity of the ISZ (Fig. 2). The Isortoq belt is located along the southeast-dipping ISZ, whereas the Eqe Bay belt is located subparallel to and ~25 km southeast of the ISZ (Jackson et al. 1978; Morgan 1982). Both greenstone belts consist of a lower metavolcanic package containing iron formation that is unconformably overlain by metaconglomerate, followed by a sequence of finer grained siliciclastic rocks (e.g., metagraywacke, metasiltstone, quartzite; Bethune and Scammell 1997). Eqe Bay strata are less metamorphosed (~greenschist to lower amphibolite) than Isortoq strata (~upper amphibolite to granulite), with the former retaining primary sedimentary and volcanic features. Both greenstone belts are nonetheless polydeformed, analogous to observations of Mary River Group occurrences elsewhere on northern Baffin Island (Young et al. 2004; Bros and Johnston 2017; Saumur et al. 2018).

Mapping north of latitude 70°N (Skipton et al. 2020a, b) across and on both sides of the ISZ (Fig. 1B) revealed a discontinuous shear zone (e.g., mylonite was not observed along transect IQ-B, Fig. 1B). An aeromagnetic boundary between rocks southeast of the ISZ, which exhibit a lower magnetic susceptibility (<0.05 SI) from those to the northwest (>0.1 SI and up to ~10 SI), is readily observed in regional aeromagnetic surveys (Fig. 1B) and is likely attributable to a lithological boundary. Structurally lower, more magnetic rocks to the NW correspond broadly to OPX-bearing felsic gneisses of the Dexterity Bay granulite belt. These are overlain to the SSE of the ISZ by non-OPX-bearing monzogranitic to granodioritic plutons. The plutons exhibit a variably developed, locally lineated, gneissic foliation that parallels the contact, although fabrics tend to become shallower southeast of the shear zone (Fig. 1B). Narrow (10 metre wide), discontinuous and discrete mylonite zones characterised by down-dip (top-to-the-SSE) shearing are common along the lithological boundary. The mylonites are characterised by a variably developed SE-plunging stretching lineation defined primarily by elongate quartz-feldspar aggregates. S-C and S-C-C' fabrics (Fig. 3A) are consistent with down-dip, top-to-the-SSE shearing. These observations suggest that there is no single continuous ISZ, and hence no suture or major crustal discontinuity along the shear zone. Instead, the ISZ constitutes a reworked and strained primary contact between two distinct meta-igneous units.

The gneissic fabric that characterises the Isortoq belt is folded. The folds (Fig. 3B) are asymmetric, with short, sub-vertical, thickened limbs separating elongate, shallowly SE-dipping, thinned limbs, and record clockwise rotation (viewed looking down plunge to the NE, Fig. 3B inset). In ISZ mylonite zones, such folds are commonly developed, with strongly developed stretching lineations and mylonite characterising the thinned, SE-dipping limbs. The folds and mylonites consistently indicate top-to-the-south, normal shear sense with an apparent dextral component. Mylonite zones, though present (Jackson 2000), are sparse and discontinuous (e.g., mylonite was not observed along transect IQ-B, Fig. 1B). Mylonitic Qtz-Pl-Bt schists (e.g., along transect IQ-A) are locally characterised by mm- to cm-scale, SE-plunging crenulations (Fig. 3D). Hence there are two main groups of lineations: fold-axis parallel intersection and mineral lineations plunge NE, and are orthogonal to SE-plunging stretching and crenulation lineations (Fig. 4A).

The Mary River Group occurs sparsely along the ISZ north of 70°N, forming stretched 1-100 metre thick panels elongated parallel to the ISZ (Fig 2; Fig. 3C). South of 70°N, detailed 1:50,000-scale mapping (Bethune and Scammell 1997) shows a continuous Isortoq belt consisting of 1-10 km scale panels of Mary River Group (Figs. 1B, 2). In general, the Mary River Group panels widen, and become more continuous and spatially extensive from northeast to southwest. Structural data compiled by Bethune and Scammell (1997) show a cluster of NE-plunging fold axes, and another cluster plunging SE (Fig. 4B, left stereonet). Our mapping suggests that NNW and E plunging lineations (Fig. 4B, right stereonet) are attributable to counter clockwise block rotation about a NE-plunging axis of rotation during normal slip along an ISZ-related SE-dipping shear zone, resulting in reorientation of the NE and SE-plunging lineations that are characteristic of the belt.

The disconformity within the Mary River Group between the lower metavolcanic package and the stratigraphically overlying metaconglomerate provides a means of determining the local way up, and indicates that the regionally moderately SE-dipping Isortoq belt is overturned, younging structurally down-section towards the NW. Piling Group strata crop out northwest of the Mary River Group stata, dip homoclinally to the SE beneath the SE-dipping Mary River strata, and together with the Mary River Group define a thick, downward younging, overturned panel. The thick overturned sequence of Piling Group marble and garnet-schist (Fig. 2; Jackson et al. 1978; Morgan 1982; Skipton et al. 2020a) represents the northernmost occurrence of Piling Group, cropping out ~100 km northwest of correlative exposures in the Foxe Fold Belt. Piling Group panels NW of the Isortoq belt follow an arcuate bend that closes towards the northeast (Fig. 2) and is consistent with the local structural grain as well as the geometry of aeromagnetic anomalies. Jackson and Berman (2000) interpreted this geometry of Piling Group to be "related to dextral thrusting of the Isortoq Fault Zone". Although we did not detect evidence of thrusting along the ISZ, apparent dextral-sense motion associated with the ISZ is consistent with our observations.

Eqe Bay Greenstone Belt and Grant-Suttie Bay islands

The sub-vertical, NE-striking Eqe Bay belt (Fig. 5) comprises the least metamorphosed and best preserved portion of the Mary River Group (Bethune and Scammell 2003a, b; c.f. Skipton et al. 2017; Bros and Johnston 2017), containing well preserved pillow basalts (Fig. 5A; c.f. dismembered panels of the Isortoq belt, Fig. 3C) and continuous km-scale banded iron formation which broadly defines a 100 metre scale Z-fold (Fig. 2). Coeval perpendicular linear fabrics are spatially and genetically associated with the latter fold (Fig. 5C). A SE younging direction - opposite from that of the Isortoq belt - is inferred from pillow-tops, stratigraphic relationships, and the orientation of the disconformity between the metavolcanics and stratigraphically overlying metasedimentary (conglomeratic) rocks (Bethune and Scammell 1997). Metamorphism is indicated by the presence of chloritic greenschist in metavolcanics and by biotite-muscovite schist in metapelites. The schistose fabric is folded. Shallowly NE-plunging folds occur at all scales from thin-section up to map-scale and are characterised by vertical to steeply S-dipping long limbs, and sub-horizontal to S-dipping short limbs that are commonly thinned or sheared, yielding an asymmetric Z-geometry when viewed down plunge to the NE (Fig. 5B).

The offshore geology to the southwest of the Isortoq and Eqe Bay belts including, as exposed on the islands of Grant-Suttie Bay, imply continuity of the two belts around a synformal fold hinge (Fig. 2). Consistent with observations along the ISZ, Mary River Group rocks in Grant-Suttie Bay form discrete NE-SW striking panels (Fig. 2 inset) within strongly foliated to gneissic and locally migmatitic granodioritic to tonalitic rocks. Two perpendicular lineations characterise the gneiss (Fig. 6A): a shallowly north-northeast plunging mineral lineation (consistent with the regional fold axis), and a southeast-plunging stretching lineation (Fig. 6B). Locally, a SE-plunging crenulation lineation parallels the stretching lineation and is spatially associated with steeply SW-dipping to near-vertical quartz veins oriented perpendicular to the NNE-plunging mineral lineation. On one of the Grant-Suttie Bay islands, 50m-scale panels of amphibolite define megascopic S-folds (viewed down plunge to the NE, Fig. 6C), a parasitic geometric element consistent with a fold closure within the bay. Regional gravity data (Fig. 6D) define an arcuate pattern within Grant-Suttie Bay, which is also consistent with the presence of a fold closure at that location.

The Isortoq and Eqe belts intersect in the vicinity of Ignerit Point and Imiliq Island (Fig. 2). Greenstones on Imiliq Island (mapped by Bethune and Scammell 1997 as Mary River Group) strike NNW. Granitic rocks on Ignerit Point also strike NNW, dip shallowly to the ENE and are characterised by a subhorizontal to weakly SE-plunging stretching lineation (Fig 6B). The shallowly ENE-dipping foliations at Ignerit Point are consistent with orientations expected in the hinge of a NE-plunging synform defined by the intersection of Isortoq and Eqe fold limbs.

Discussion

Evidence for a south-verging Nappe

Structural data (Figs. 1B, 4, 5D, 6B), regional gravity surveys (Fig. 6D), stratigraphy constraints and the observed map pattern suggest that the overturned Isortoq belt is continuous with the steeply-dipping Eqe Bay greenstone belt, forming two limbs of a single folded belt (Figs. 7A-B). An arcuate plunging-inclined fold hinge joins the two belts/limbs within Grant-Suttie Bay. The fold plunges shallowly to the NE, and is characterised by a moderately inclined, ENE-striking, SSE-dipping axial surface.

Viewed down-plunge, the Isortoq and Eqe limbs are characterised by S and Z folds, respectively (Fig. 7A). The shallowly to moderately SE-dipping northerly Isortoq limb is thinned, more highly metamorphosed, sheared (Isortoq Shear Zone) and overturned (younging to the NW). Thinning of the Isortoq limb of the fold was accommodated in part by the development of a network of brittle-ductile mylonitic shear zones collectively recognized as the ISZ (Fig. 7B). The strands of the ISZ dip more steeply southeast than Isortoq Belt, are characterised by top-to-the-southeast normal sense shear, and cut stratigraphically up-section through the overturned Mary River Group strata in the direction of transport (Fig. 7B). The Caribou Fault, a normal-sense brittle fault within the Isortoq Belt that was identified by Bethune and Scammell (2003b), is interpreted as a discrete brittle strand of the ISZ and nicely exemplifies the characteristics illustrated above. The fault dips more steeply to the southeast than the overturned SE-dipping footwall strata, is characterised by down-dip to the southeast vergence, and cuts stratigraphically up-section through the overturned footwall strata in the direction of transport. The Caribou Fault appears to have transected the hinge of a map-scale parasitic fold as it preserves steeply dipping strata characterised by Z-folds in its hangingwall (Fig. 7C). A thrust or overturned thrust interpretation for the ISZ can be ruled out, as it would require that the ISZ dip more shallowly than foliation and cut stratigraphically down-section in the direction of transport through the overturned strata (Fig. 7D).

In contrast to the Isortoq limb, the sub-vertical to steeply SSE-dipping southerly Eqe limb is structurally thickened, less metamorphosed and little sheared, vertical to steeply SE-dipping, and SE-facing (Fig. 7A). An arcuate hinge zone connecting the two limbs lies mostly unexposed beneath the waters of Grant-Suttie Bay (Figs. 2, 6). Together, the two limbs and the connecting hinge zone define a fold that we interpret as a synformal anticline based on younging directions radiating away from the fold's core. This interpretation is consistent with occurrences of panels of Piling Group NW of the Isortoq belt (Fig. 2), as well as in the Foxe Fold Belt to the SE. Folds with subparallel axial traces and similar geometries, occurring to the southeast of Eqe Bay near Gillian Lake (St-Onge et al. 2006), are likely part of the same structure (Fig. 2).

We propose that these folds form part of a larger-scale nappe ("Isortoq Nappe" hereafter), and that the Grant-Suttie Bay area expose a portion of the lower overturned limb of a south-verging nappe (Fig. 7A). Southward vergence is consistent with the geometry of the belt-scale synformal anticline, the well-developed stretching lineations, and extensive top-to-the SE shearing of the Isortoq limb. Several structural elements considered characteristic of nappes (Fig. 8; e.g., Bastida et al. 2014) are documented in the Grant-Suttie Bay area, including (1) synformal anticlines and antiformal synclines along the nappe's overturned lower limb (Fig. 7A); (2) asymmetric, mesocopic-scale, parasitic folds that verge in the opposite direction of nappe emplacement and which are characterised by a thinned and extended overturned limb and a structurally thickened, upright, short limb (Fig. 3B); and (3) perpendicular coeval linear elements: a fold axis parallel lineation, a stretching lineation that records the transport direction of the nappe (Fig. 8). NW-plunging stretching lineations (Fig. 4B) could also be locally expected due to progressive rotation of layers during the advance of a nappe (Fig. 8, bottom right inset). Crenulations and quartz veins parallel to the transport direction and perpendicular to the fold axis are known to form as a result of lateral spreading of the nappe (Fig. 8; Ratschbacher et al. 1989; Zhang et al. 2000; Davis and Maidens 2003); thus local variability of ISZ fabrics (ex. Fig. 3D) can be attributed to later stage lateral spreading during nappe emplacement.

Implications for the Trans-Hudson Orogen: a link to the Rinkian Belt?

Given the distribution and structural grain of panels of Piling group NW of the study area (Figs. 1B, 2), Piling group is interpreted to be involved in the deformation associated with the emplacement of the Isortoq Nappe. The involvement of Piling Group strata implies that deformation was syn- to post-Paleoproterozoic, and likely a product of the THO (e.g. St-Onge et al. 2009). THO-aged tectonism in the Isortoq area is further supported by U-Pb metamorphic ages of ca. 1.85-1.82 Ga (Bethune and Scammell 2003b). The south-vergence of the Isortoq nappe contrasts with the north to northwest vergence of the THO-related Foxe Fold Belt exposed immediately south, as well as north-verging Nagssugtoqidian deformation in Greenland (e.g., Jackson and Berman 2000; St-Onge et al. 2009; Sanborn-Barrie et al. 2014). SW-verging nappes have been documented along the northeastern coast of Baffin Island (Jackson and Berman 2000). Some of these nappes, including the Pilattuaq Nappe (see figure 5 of Jackson and Berman 2000, known as Scott Island Nappe), ~260 km NE of Grant-Suttie Bay (Fig. 1A), occur along-strike from and are characterised by the same broad S-transport direction as the Isortoq Nappe.

Jackson and Berman (2000) proposed that such structural elements of NE Baffin could be the extension of the south-verging early Rinkian fold belt of west Greenland (Kalsbeek 1986; Grocott and Pulvertaft 1990), which was adjacent to Baffin Island prior to the Cretaceous opening of Baffin Bay and Davis Strait (e.g. St-Onge et al. 2009). The

Rinkian fold belt represents an early deformation phase of the THO, characterised by WSW-verging transport (Grocott and McCaffrey 2017) that preceded the N-verging deformation characterising later phases of the THO (Henderson et al. 1989). Our work therefore suggests that the Rinkian deformation phase extends much further, across the entirety of Baffin Island. This highlights and significantly extends the strike-length of a south-verging nappe front distinct from subsequent north-verging nappes of the Foxe fold belt.

Conclusion

Geophysical surveys highlight the occurrence of the ISZ, despite its cryptic nature in the field. Contrary to previous interpretations, we do not consider this structure as a major thrust fault separating Archean crustal blocks. Instead, structural and stratigraphic evidence suggest that it represents a shear zone within the overturned lower limb of a S-verging Trans-Hudsonian nappe. Consistent with vergence directions observed in Greenland, initial vergence directions during collision were southward, and were later overprinted by north-verging deformation such as that observed in the Foxe Fold belt. Our findings thus have implications for our understanding of the tectonic framework of the northeastern Trans-Hudson Orogen. Furthermore, the significant spatial extent of the Isortoq nappe highlights the importance of horizontal transport during the Paleoproterozoic and the construction of the Nuna Supercontinent.

The Isortoq nappe was characterised through the identification of structural elements that are typical of collisional geodynamic environments. Despite the availability of regional geophysical surveys, the nappe could not have been identified in such deeply eroded terranes without boots-on-the-ground fieldwork. In addition, Canada's Arctic remains difficult to access and relatively unexplored. Our study, like many others conducted in polydefomed remote terranes, highlights that many secrets remain to be discovered in vast, geologically unchartered territories.

Acknowledgements

This work partly includes observations stemming from the Natural Resources Canada (NRCan) Geomapping for Energy and Minerals program (GEM-2) North Baffin Bedrock Mapping activity (2017-18). The Polar Continental Shelf Program and the Tuniniq Sauniq Co-Op (Pond Inlet) provided logistical support during the 2017-18 field mapping campaigns. BMS and STJ thank John Hey, Luke Howitt and Tom Iannelli (Baffinland Iron Mines) for their support and invitation to participate in the Eqe Bay exploration programs of 2019 and 2021. BMS and STJ are supported by National Science and Engineering Research Council Discovery Grants RGPIN-2021-03306 and RGPIN-2019-04275, respectively.

References

Bastida, F., Aller, J., Fernández, F.J., Lisle, R.J., Bobillo-Ares, N.C., and Menendez, O., 2014. Recumbent folds: key structural elements in orogenic belts. Earth-Science Reviews, **135**: 162-183. https://doi.org/10.1016/j.earscirev.2014.05.002

Beauchemin, M., Tschirhart, V., Harris, J., and Lamontagne, M., 2019. A method for curvilinear structure mapping in normalized derivative magnetic maps. Journal of Applied Geophysics, **162**: 72-79 https://doi.org/10.1016/j.jappgeo.2018.10.002

Bethune, K.M., and Scammell, R.J. 1997a. Precambrian geology, Koch Island area (part of NTS 37C), District of Franklin, Northwest Territories. Geological Survey of Canada, Open File 3391, 4 sheets, CD-ROM, https://doi.org/10.4095/208509

Bethune, K.M., and Scammell, R.J., 2003a. Geology, geochronology, and geochemistry of Archean rocks in the Eqe Bay area, north-central Baffin Island, Canada: constraints on the depositional and tectonic history of the Mary River Group of northeastern Rae Province. Canadian Journal of Earth Sciences, **40**: 1137–1167. https://doi.org/10.1139/e03-028

Bethune, K.M., and Scammell, R.J., 2003b. Distinguishing between Archean and Paleoproterozoic tectonism, and evolution of the Isortoq fault zone, Eqe Bay area, north-central Baffin Island, Canada. Canadian Journal of Earth Sciences, **40**: 1111–1135. https://doi.org/10.1139/e03-040

Bros, E.R., and Johnston, S.T., 2017. Field observations of the Mary River Group south of Tay Sound, northern Baffin Island, Nunavut: stratigraphy and structure of supracrustal sequences and surrounding plutonic units. *In:* Summary of Activities 2017, Canada-Nunavut Geoscience Office, 69–80.

Corrigan, D., Pehrsson, S., Wodicka, N., and de Kemp, E., 2009. The Palaeoproterozoic Trans-Hudson Orogen: a prototype of modern accretionary processes. Geological Society, London, Special Publications, **327**: 457-479. https:// DOI:10.1144/SP327.19

Davis, B.K., and Maidens, E., 2003. Archaean orogen-parallel extension: evidence from the northern Eastern Goldfields Province, Yilgarn Craton. Precambrian Research, **127**: 229-248. https:// DOI:10.1016/S0301-9268(03)00189-X

Friend, C.R.L., and Nutman, A.P., 1991. Refolded nappes formed during late Archaean terrane assembly, Godthabs fjord, southern West Greenland. Journal of the Geological Society, London, **148**: 507-519. https://DOI:10.1144/gsjgs.148.3.0507

Gagné, S., Jamieson, R.A., MacKay, R.,Wodicka, N., and Corrigan, D., 2009. Texture, composition, and age variations in monazite from the lower amphibolite to the granulite facies, Longstaff Bluff Formation, Baffin Island, Canada. Canadian Mineralogist, **47**: 847–869. http://dx.doi.org/10.3749/canmin.47.4.847

Grocott, J., and McCaffrey, K.J.W., 2017. Basin evolution and destruction in an Early Proterozoic continental margin: the Rinkian fold–thrust belt of central West Greenland, Journal of the Geological Society, London, **174**: 453-467. https://doi.org/10.1144/jgs2016-109

Grocott, J., and Pulvertaft, T.C.R., 1990. The early Proterozoic Rinkian belt of central West Greenland. Geological Association of Canada, Special Paper, **37**: 443-463.

Harrison, J.C., Saumur, B.M., and Skipton, D.R., 2022. Mineral and carving-stone resources of Baffin Island, Nunavut (Chapter 13). *In:* Dafoe, L.T. and Bingham-Koslowski, N. (eds.) Geological synthesis of Baffin Island (Nunavut) and the Labrador-Baffin Seaway; Geological Survey of Canada, Bulletin 608.

He, J., Harris, J.R., Sawada, M., Behnia, P.et al., 2015. A comparison of classification algorithms using Landsat-7 and Landsat-8 data for mapping lithology in Canada's Arctic. International Journal of Remote Sensing, **36**: 2252-2276. https://doi.org/10.1080/01431161.2015.1035410

Henderson, J.R., and Tippett, C.R., 1980. Foxe Fold Belt in eastern Baffin Island, District of Franklin. Geological Survey of Canada, Paper 80-1A, 147-152. https://doi.org/10.4095/106195

Henderson, J.R., Grocott, J., Henderson, M.N., and Perrault, S., 1989. Tectonic history of the Lower Proterozoic Foxe-Rinkian Belt in central Baffin Island, N.W.T., Geological Survey of Canada, Paper 89-1C, 185-197. https://doi.org/10.4095/126852

Hoffman, P.F., 1988. United Plates of America, the birth of a craton: Early Proterozoic assembly and growth of Laurentia. Annual Review of Earth and Planetary Sciences, **16**: 543–603. https://doi.org/10.1146/annurev.ea.16.050188.002551

Jackson, G.D., Morgan, W.C., and Davidson, A., 1978. Geology, Steensby Inlet, District of Franklin. Geological Survey of Canada, Map 1450A, coloured, with expanded legend, scale 1:250 000. https://doi.org/10.4095/109160

Jackson, G.D., and Morgan, W.C., 1978. Geology, Conn Lake, District of Franklin. Geological Survey of Canada, Map 1458A, coloured, with expanded legend, scale 1:250 000. https://doi.org/10.4095/109162

Jackson, G.D., Hunt, P.A., Loveridge, W.D. and Parrish, R.R., 1990. Reconnaissance geochronology of Baffin Island, N.W.T. In Radiogenic Age and Isotopic Studies: Report 3, Geological Survey of Canada, 89-2, 123-148. https://doi.org/10.4095/129079

Jackson, G.D., 2000. Geology of the Clyde-Cockburn Land map area, north-central Baffin Island, District of Franklin. Geological Survey of Canada, Memoir 440, 316 pp. (6 sheets). https://doi.org/10.4095/211268

Jackson, G.D., and Berman, R.G., 2000. Precambrian metamorphic and tectonic evolution of northern Baffin Island, Nunavut, Canada. Canadian Mineralogist, **38**: 399–421. https://doi.org/10.2113/gscanmin.38.2.399

Jackson, G.D., and Taylor, F.C., 1972. Correlation of major Aphebian rock units in the northeastern Canadian Shield. Canadian Journal of Earth Sciences, **9**: 1650-1669, https://doi.org/10.1139/e72-146

Kalsbeek, F., 1986. The tectonic framework of the Precambrian shield of Greenland, a review of new isotopic evidence. In Kalsbeek, F. and Watt, W.S.: Developments in Greenland Geology. Grønlands Geol. Unders., Rapp., **128**: 55-64.

Lebeau, L.E., Russer, M, Therriault, I, Bovingdon, P.J., Dufour, F., Greenman, J.W., and Patzke M., 2019. Regional Precambrian bedrock mapping of the Jungersen River area, northwestern Baffin Island, Nunavut. *In:* Summary of Activities 2019, Canada-Nunavut Geoscience Office, 49–68.

Lewry, J.F., and Collerson, K.D., 1990. The Trans-Hudson Orogen: extent, subdivisions and problems. in: Lewry, J.F., Stauffer, M.R. (eds.), The Early Proterozoic Trans-Hudson Orogen of North America. Geological Association of Canada, Special Paper **37**: 1-14.

McClay, J.C., and Price, N.J., 1981. Thrust and Nappe Tectonics. Geological Society of London Special Publication **9**, 539 pp.

Morgan, W.C., Okulitch, A.V., and Thompson, P.H., 1976. Stratigraphy, Structure and Metamorphism of the West Half of the Foxe Fold Belt, Baffin Island. Geological Survey of Canada, Paper 76-1B, 387-391. https://doi.org/10.4095/104230.

Morgan, W.C., 1982. Geology, Koch Island, District of Franklin. Geological Survey of Canada “A” Series Map 1535A, 1 sheet. https://doi.org/10.4095/127056

Miles, W., and Oneschuk, D., 2016. Magnetic anomaly map, Canada / Carte des anomalies magnétiques, Canada. Geological Survey of Canada Open File 7799. https://doi.org/10.4095/297337

Natural Resources Canada, 2020. Canadian Airborne Geophysical Data Base, Airborne Geophysics Section, Geological Survey of Canada, Lands and Minerals Sector, Natural Resources Canada. http://gdr.agg.nrcan.gc.ca/gdrdap/dap/search-eng.php [May 2020].

Partin, C.A., Bekker, A., Corrigan, D., Modeland, S., Francis, D., and Davis, D.W., 2014. Sedimentological and geochemical basin analysis of the Paleoproterozoic Penrhyn and Piling groups of Arctic Canada. Precambrian Research, **251**: 80-101. https://doi.org/10.1016/j.precamres.2014.06.010

Pehrsson, S.J., Berman, R.G., Eglington, B., and Rainbird, R.H., 2013. Two Neoarchean supercontinents revisited: the case for a Rae family of cratons. Precambrian Research, **232**: 4-26. https://doi.org/10.1016/j.precamres.2013.01.021

Rainbird, R.H., Davis, W.J., Pehrsson, S.J., Wodicka, N., Rayner, N., and Skulski, T., 2010. Early Paleoproterozoic supracrustal assemblages of the Rae domain, Nunavut, Canada: Intracratonic basin development during supercontinent break-up and assembly. Precambrian Research, **181**: 167-186. https://doi:10.1016 /j.precamres.2010.06.005.

Ramsay, J.G., 1981. Tectonics of the Helvetic nappes. Geological Society, London, Special Publications, **9**: 293-309.

Ratschbacher, L., Frisch, W., Neubauer, F., Schmid, S.M., and Neugebauer, J. 1989. Extension in compressional orogenic belts: The eastern Alps. Geology **17**: 404–407. https://doi.org/10.1130/0091-7613(1989)017

Saumur, B.M., Skipton, D.R., St-Onge, M.R., Bros, E.R., Acosta-Gongora, P., Kelly, C.J., Morin, A., O'Brien, M.E., Johnston, S.T., and Weller, O.M., 2018. Precambrian geology of the surroundings of Steensby Inlet and western Barnes Ice Cap (parts of NTS 37E, 37F, 37G), Baffin Island, Nunavut. *In:* Summary of Activities 2018, Canada-Nunavut Geoscience Office, 27-45.

Sanborn-Barrie, M., Davis, W.J., Berman, R.G., Rayner, N., Skulski, T., and Sandeman, H., 2014. Neoarchean continental crust formation and Paleoproterozoic deformation of the central Rae craton, Committee Bay belt, Nunavut. Canadian Journal of Earth Sciences, **51**: 635-667. https://doi.org/10.1139/cjes-2014-0010

Scott, D.J., St-Onge, M.R., and Corrigan, D., 2002. Geology of the Paleoproterozoic Piling Group and underlying Archean gneiss, central Baffin Island, Nunavut. Geological Survey of Canada, Paper 2002-C17, 10 p. https://doi.org/10.4095/213194.

Scott, D.J., St-Onge, M.R., and Corrigan, D., 2003. Geology of the Archean Rae Craton and Mary River Group and the Paleoproterozoic Piling Group, central Baffin Island, Nunavut. Geological Survey of Canada, Paper 2003-C26, 12 p. https://doi.org/10.4095/214208

Snyder, D.B., Berman, R.G., Kendall, J.-M., and Sanborn-Barrie, M., 2013. Seismic anisotropy and mantle structure of the Rae craton, central Canada, from joint interpretation of SKS splitting and receiver functions. Precambrian Research, **232**: 189-208, https://doi.org/10.1016/j.precamres.2012.03.003

Skipton, D.R., Saumur, B.M., St-Onge, M.R., Wodicka, N., Bros, E.R., Morin, A., Brouillette, P., Weller, O.M., and Johnston, S.T. 2017. Precambrian bedrock geology of the Pond Inlet–Mary River area, northern Baffin Island, Nunavut. *in:* Summary of Activities 2017, Canada-Nunavut Geoscience Office, 49–68.

Skipton, D.R., Wodicka, N., McNicoll, V., Saumur, B.M., St-Onge, M.R., and Young, M.D., 2019. U-Pb zircon geochronology of Archean greenstone belts (Mary River Group) and surrounding Archean to Paleoproterozoic rocks, northern Baffin Island, Nunavut. Geological Survey of Canada, Open File 8585, 1 .zip file. https://doi.org/10.4095/314938

Skipton, D.R., Saumur, B.M., St-Onge, M.R., Bros, E.R., Acosta-Gongora, P., Kelly, C.J., O'Brien, M.E., Weller, O.M., and Johnston, S.T., 2020a. Bedrock Geology, Barnes Ice Cap Northwest, Nunavut, NTS 37E west. Canadian Geoscience Map 402, 1 sheet, https://doi.org/10.4095/314657

Skipton, D.R., Saumur, B.M., St-Onge, M.R., Bros, E.R., Acosta-Gongora, P., Kelly, C.J., O'Brien, M.E., Johnston, S.T., and Weller, O.M., 2020b. Bedrock Geology, Rowley River – Isortoq River, Nunavut, NTS 37F east. Canadian Geoscience Map 406, 1 sheet, https://doi.org/10.4095/315401

St-Onge, M.R., Searle, M.P., and Wodicka, N., 2006. Trans-Hudson Orogen of North America and Himalaya-Karakoram-Tibetan Orogen of Asia: Structural and thermal characteristics of the lower and upper plates. Tectonics **25**: TC4006, 22 p. https://doi.org/10.1029/2005TC001907

St-Onge, M.R.; Scott, D.J.; Rayner, N.; Sanborn-Barrie, M.; Skipton, D.R.; Saumur, B.M.; Wodicka, N., and Weller, O.M., 2020, Archean and Paleoproterozoic cratonic rocks of Baffin Island [advance contribution], in Dafoe, L.T. and Bingham-Koslowski, N. (eds.)

Geological synthesis of Baffin Island (Nunavut) and the Labrador-Baffin Seaway; Geological Survey of Canada, Bulletin 608, 1-29. https://doi.org/10.4095/321824

St-Onge, M.R., Scott, D.J., Corrigan, D., and Wodicka, N., 2006, Geology, Ikpik Bay, Geological Survey of Canada, "A" Series Map 2077A, 1 sheet; 1 CD-ROM, https://doi.org/10.4095/221054

St-Onge, M.R., Van Gool, J.A.M., Garde, A.A., and Scott, D.J., 2009. Correlation of Archean and Paleoproterozoic units between northeastern Canada and western Greenland: constraining the pre-collisional upper plate accretionary history of the Trans-Hudson Orogen. Geological Society of London Special Publication **318**: 193-235. https://doi.org/10.1144/SP318.7

Steenkamp, H.M., Bovingdon, P.J., Dufour, F., Généreux, C.-A., Greenman, J.W., Halverson, G.P., Ielpi, A., Patzke M., and Tinkham, D.K., 2018. New regional mapping of Precambrian rocks north of Fury and Hecla Strait, northwestern Baffin Island, Nunavut. in: Summary of Activities 2018, Canada-Nunavut Geoscience Office, 47-62.

Weller, O.M., and St-Onge, M.R., 2017. Record of modern-style plate tectonics in the Palaeoproterozoic Trans-Hudson Orogen. Nature Geoscience, **10**: 305–311. https://doi:10.1038/ngeo2904

Weller, O., Mottram, C., St-Onge, M.R., Möller, C., Strachan, R., Rivers, T., Copley, A., 2021. The metamorphic and magmatic record of collisional orogens. Nature Reviews Earth and Environment, 19 p., https://doi.org/10.1038/s43017-021-00218-z.

de Wit, M.J., 1982. Gliding and overthrust nappe tectonics in the Barberton Greenstone Belt. Journal of Structural Geology, **4**: 117-136. https://doi.org/10.1016/0191-8141(82)90022-0

Wodicka, N. St-Onge, M.R., Corrigan, D., Scott, D.J., and Whalen, J.B., 2014. Did a proto-ocean basin form along the southeastern Rae cratonic margin? Evidence from U-Pb geochronology, geochemistry (Sm-Nd and whole-rock), and stratigraphy of the Paleoproterozoic Piling Group, northern Canada. Geological Society of America Bulletin, **126**: 625-1653. https://doi.org/10.1130/B31028.1

Young, M.D., Sandeman, H., Berniolles, F., and Gertzbein, P.M., 2004. A preliminary stratigraphic and structural geology framework for the Archean Mary River Group, northern Baffin Island, Nunavut. Current Research (Online) 2004-C1, 14 pp. https://doi.org/10.4095/215376

Zhang, J., Ding, L., Zhong, D., and Zhou, Y., 2000. Orogen-parallel extension in Himalaya: Is it the indicator of collapse or the product in process of compressive uplift? Chinese Science Bulletin, **45**: 114–120. https://doi.org/10.1007/BF02884653

Figures

Figure 1: (A) Map of Baffin Island and the western coast of Greenland, showing the major cratonic and structural elements (ISZ: Isortoq shear zone; FFB: Foxe Fold Belt; Rae C.: Rae Craton; Meta Incg. Microc.: Meta Incognita Microcontinent; AD: Aasiaat Domain, NAC: North Atlantic Craton) **(B)** Residual-total-field aeromagnetic data for northern Baffin Island (Natural Resources Canada 2020; "Canada - 200 m - MAG"), and bedrock mapping stations along the ISZ. The aeromagnetic data were collected during 1973–1974 along flight lines spaced 805 m apart flown at an altitude of 305 m (Miles and Oneschuk 2016). Pink = 476 nT; Dark blue = -2432 nT. The highly reflective body at the bottom left corner is the Eqe Bay Iron Formation (EB BIF). GSB: Grant-Suttie Bay.

Selected bedrock mapping stations near the ISZ (dotted line, location estimated from aeromagnetic data) are identified in grey (NW of ISZ) and white (SE of ISZ); two mapping traverses discussed in the text are identified (IQ-A and IQ-B). Bottom right corner: lower hemisphere stereographic projection of poles of foliation measurements from stations NW (44 data points) and SE (37 data points) of the ISZ. Great circles associated with peak Kamb contours for each dataset are indicated.

Figure 2: Simplified geology map of the Isortoq and Eqe Bay area, from this study and previous geological mapping (1:50,000: Bethune and Scammell 1997; 1:100,000: St-Onge et al. 2006; Skipton et al. 2020a, b). Red dashed lines identify the geometry of the unexposed fold proposed in this study. Representative lineation orientations are indicated. Meso- to Neoproterozoic sedimentary rocks of the Fury and Hecla Group (FH) are exposed near Ignerit Point but are not relevant to this study. Upper left inset: updated geology of the islands of Grant-Suttie Bay.

Figure 3: Representative field photographs from the northern portion of the Isortoq Belt Shear Zone Decimetre-scale folds consistent with normal sense, top-to-the-SE shearing (see inset and text for discussion), photo facing east. **C)** Stretched metre-scale panel of amphibolite (Mary River Group), hammer for scale. Photograph facing E). **D)** Crenulated Qtz-Pl-Bt mylonite, crenulations plunge SE.

Figure 4: Linear structures of the Isortoq Belt. **A)** IQ-A traverse; **B)** Isortoq Belt data from Bethune and Scammell (1997). Lower-hemisphere stereographic projection of selected field data, see text for discussion. Ls = Stretching Lineation; Lm = Mineral Lineation; FA = Fold Axis; Crens. = Crenulations. See text for discussion.

Figure 5: Field photographs of the Eqe Bay belt (locations provided in Figure 2). **A)** An example of weakly deformed (flattened) pillow basalts. **B)** Z-fold in metasediments of the

Eqe Bay belt, with associated axial plane inclined towards the SE. **C)** Perpendicular fabrics: shallowly-NNE-plunging lineation defined by boudin necks (regional fold axis) and steeply-SSE-plunging crenulation lineation, pelitic iron formation. **D)** Lower-hemisphere stereographic projection of poles of S1 foliation data from by Bethune and Scammell (1997). Average foliation 045/87 shown with a great circle. Kamb contours shown in increments of two standard deviations.

Figure 6: Grant-Suttie Bay islands and Ignerit Point; field photographs and representative structural data (locations of photographs provided in Figure 2). **A)** Perpendicular fabrics within rocks of the ISZ; a SE-plunging crenulation lineation (yellow pencil direction) overprints a faint NE-plunging mineral lineation (parallel to the grey scribe pen). **B)** Lower-hemisphere stereographic projection; linear structural data of Grant-Suttie Islands (GSI) and Ignerit Point (IP). Ls = Stretching Lineation; Lm = Mineral Lineation; FA = Fold Axis; Crens. = Crenulations. **C)** Aerial view of northeastern tip of central Grant-Suttie Bay Island (informally known as "BIM" island) showing mesoscopically S-folded panels of amphibolite. **D)** Bouguer gravity anomaly in the Eqe Bay area (Natural Resources Canada 2020; "Canada 2 km - GRAV - Gravity Anomalies"), showing anomaly possibly related to unexposed fold core in Grant-Suttie Bay. The location of "BIM" Island (Fig. 6C) is indicated with an X. S-folds found on that island are consistent with the proposed fold geometry.

Figure 7: Summary of geometries observed in the Grant-Suttie Bay area and Isortoq Nappe model. **A)** Upper figure - Conceptual view of the Isortoq Nappe, facing down plunge, whereby the Isortoq-Eqe section represents a portion of the overturned lower limb of a S-verging nappe. Lower figure - The Isortoq and Eqe Bay belts form one continuous belt, forming an antiformal syncline, with S-folds associated with the Isortoq limb (including the Grant-Suttie islands) and Z-folds associated with Eqe Bay limb. **B)**

Oblique 3D view of the Isortoq-Eqe Bay fold, facing N, highlighting the presence of two lineations (Ls = stretching lineation; FA = fold axis, or mineral lineation). The lower panel demonstrates how the ISZ, developed as a consequence of shearing at the base of the Nappe, contributed to the dismemberment of the Isortoq Belt. **C)** The Caribou Fault is a brittle representation of the ISZ that offsets portions of Mary River Group in the Isortoq Belt. Consistent with the model presented in Fig. 7B and the mapping of Bethune and Scammell (1997), it is interpreted to cut a parasitic fold within the Nappe. Figures on the left, in section view, show incipient development of a normal-fault within folded Mary River Group (MRG); the figure on the right, after Bethune and Scammell (2003b), schematically highlights the 3D relationship observed in the Isortoq Belt; facing N. **D)** A potential alternate model, consisting of an overturned thrust, does not reproduce the mapped stratigraphic and structural relationships. See text for details.

Figure 8: Expected angular relationship between structural elements in a nappe. Main figure: viewed perpendicular to the direction of transport. Bottom right inset: viewed parallel to the nappe fold axis; NW-plunging stretching lineations are possible in portions of the overturned as the nappe rolls over. See text for discussion.

650 FIGURES

651 FIGURE 1

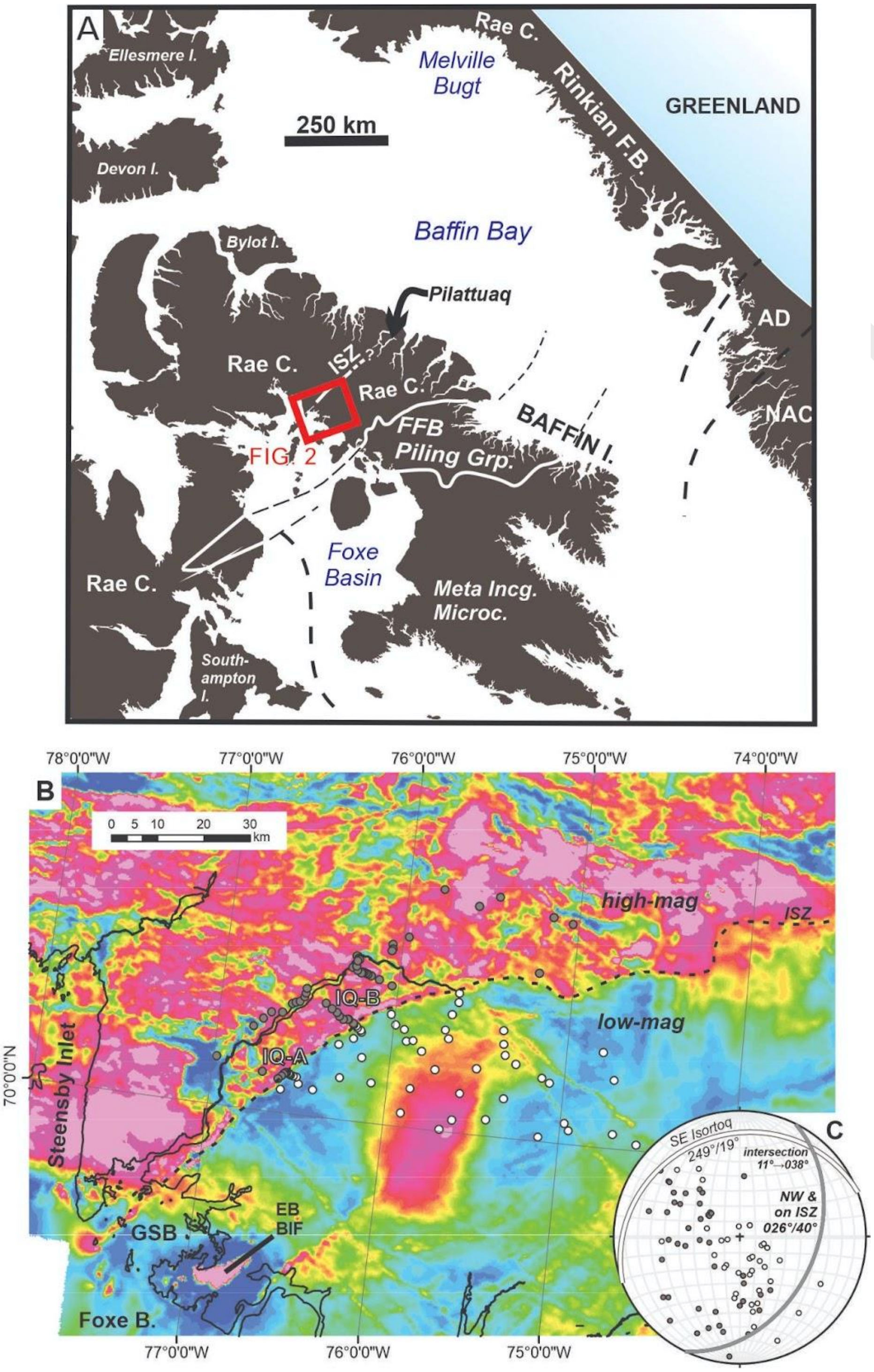

652

653

FIGURE 2

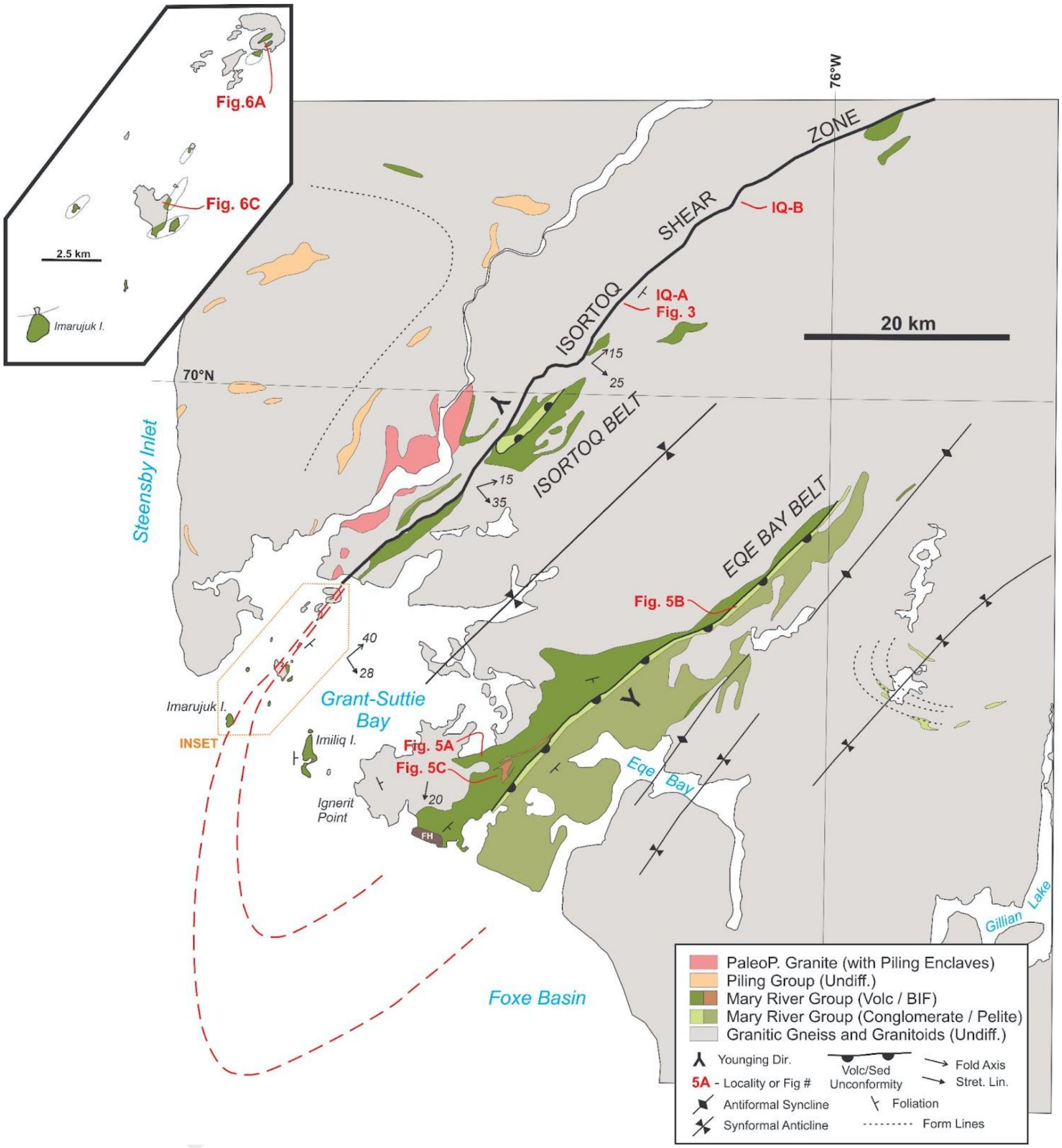
Fig.6A
Fig. 6C
2.5 km
Imarujuk I.
76°W
ZONE
SHEAR
ISORTOQ
IQ-B
IQ-A
Fig. 3
20 km
15
25
70°N
ISORTOQ BELT
15
35
Steensby Inlet
EQE BAY BELT
Fig. 5B
40
28
Grant-Suttie
Bay
Imarujuk I.
INSET
Imiliq I.
Fig. 5A
Fig. 5C
20
Ignerit
Point
FH
Eqe Bay
Gillian Lake
Foxe Basin
PaleoP. Granite (with Piling Enclaves)
Piling Group (Undiff.)
Mary River Group (Volc / BIF)
Mary River Group (Conglomerate / Pelite)
Granitic Gneiss and Granitoids (Undiff.)
Younging Dir.
Volc/Sed Unconformity
Fold Axis
Stret. Lin.
5A - Locality or Fig #
Antiformal Syncline
Foliation
Synformal Anticline
Form Lines

FIGURE 3

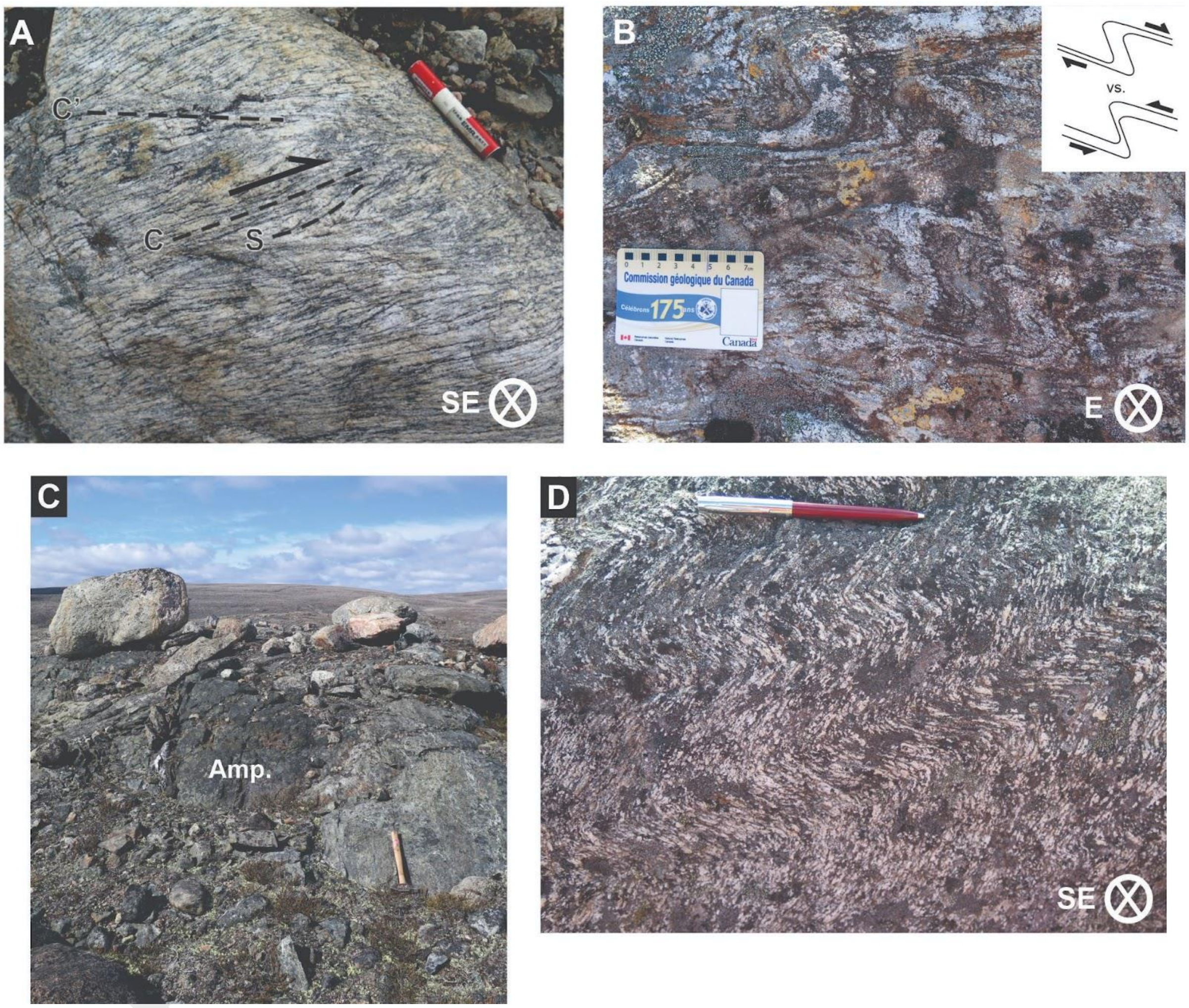
A
C'
C
S
SE
B
vs.
Commission géologique du Canada
175
Canada
E
C
Amp.
D
SE

FIGURE 4

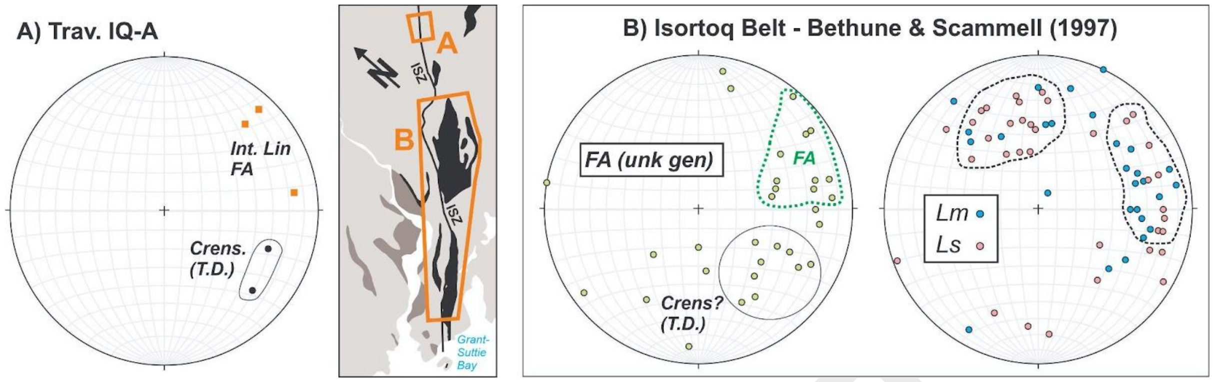
A) Trav. IQ-A
Int. Lin
FA
Crens.
(T.D.)
N
A
B
ISZ
ISZ
Grant-
Suttie
Bay
B) Isortoq Belt - Bethune & Scammell (1997)
FA (unk gen)
FA
Crens?
(T.D.)
Lm
Ls

669 FIGURE 5

670

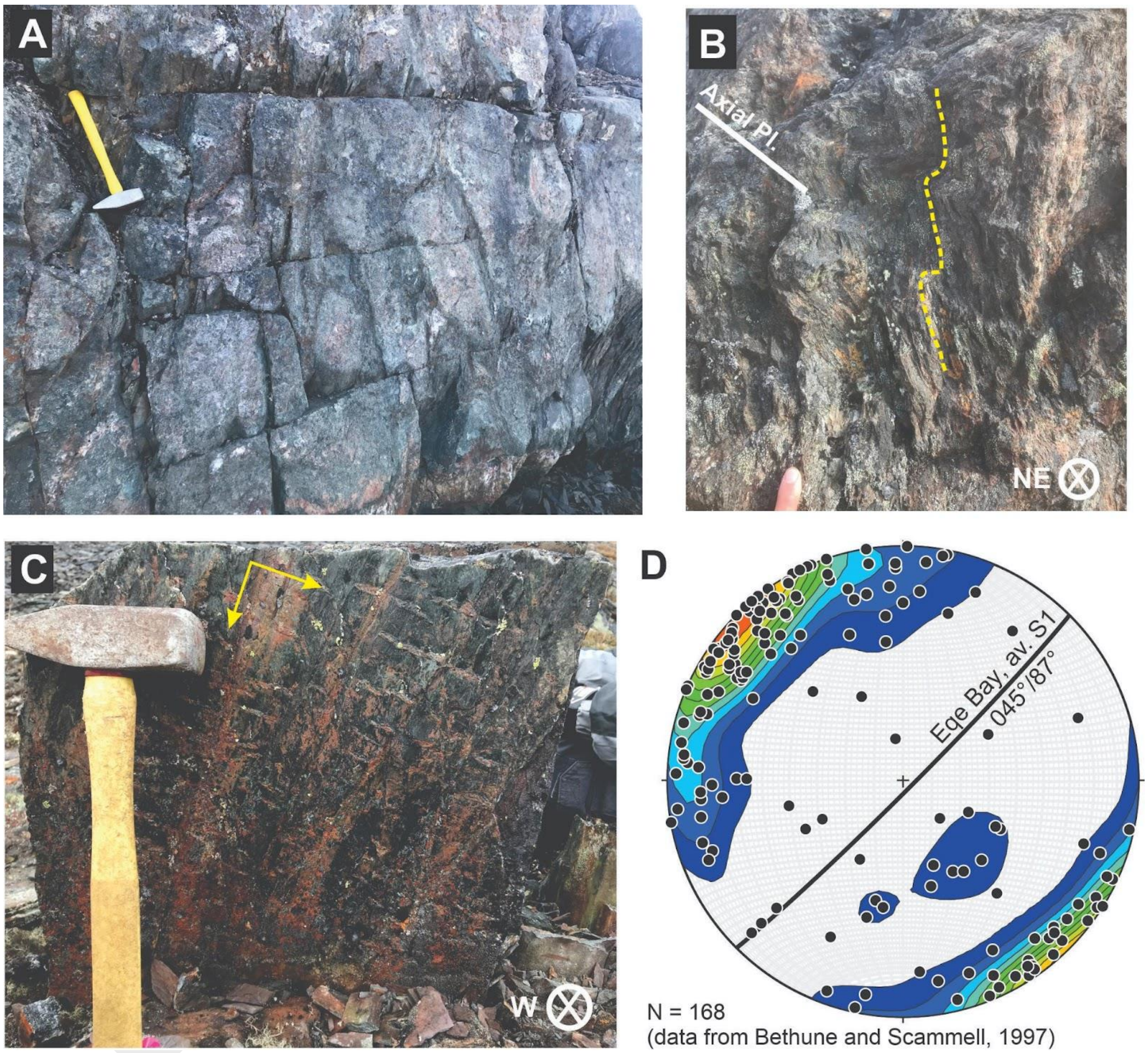

671

672

673

FIGURE 6

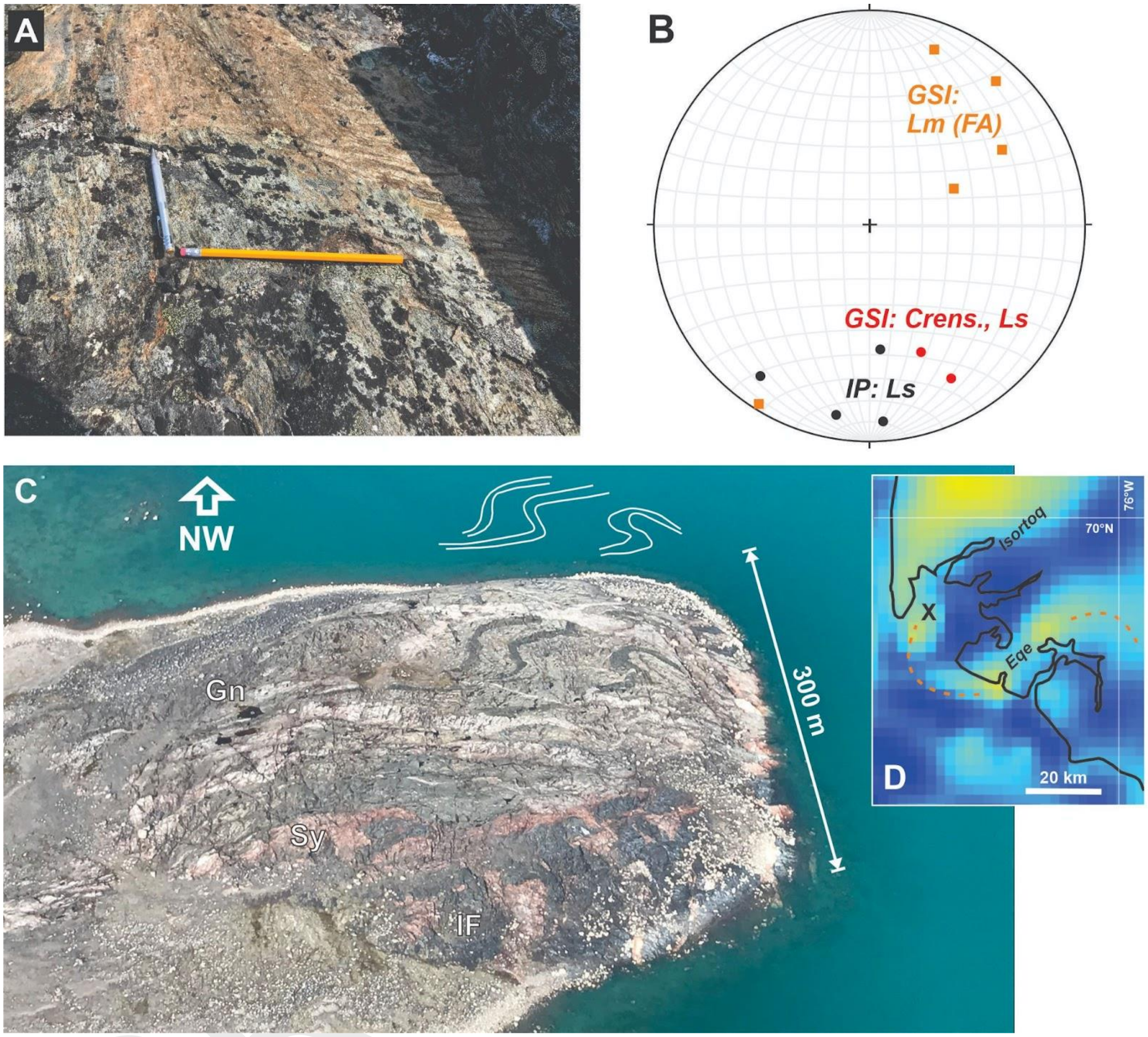
A
B
GSI:
Lm (FA)
GSI: Crens., Ls
IP: Ls
C
NW
Gn
Sy
IF
300 m
D
76°W
70°N
Isortoq
X
Eqe
20 km

FIGURE 7

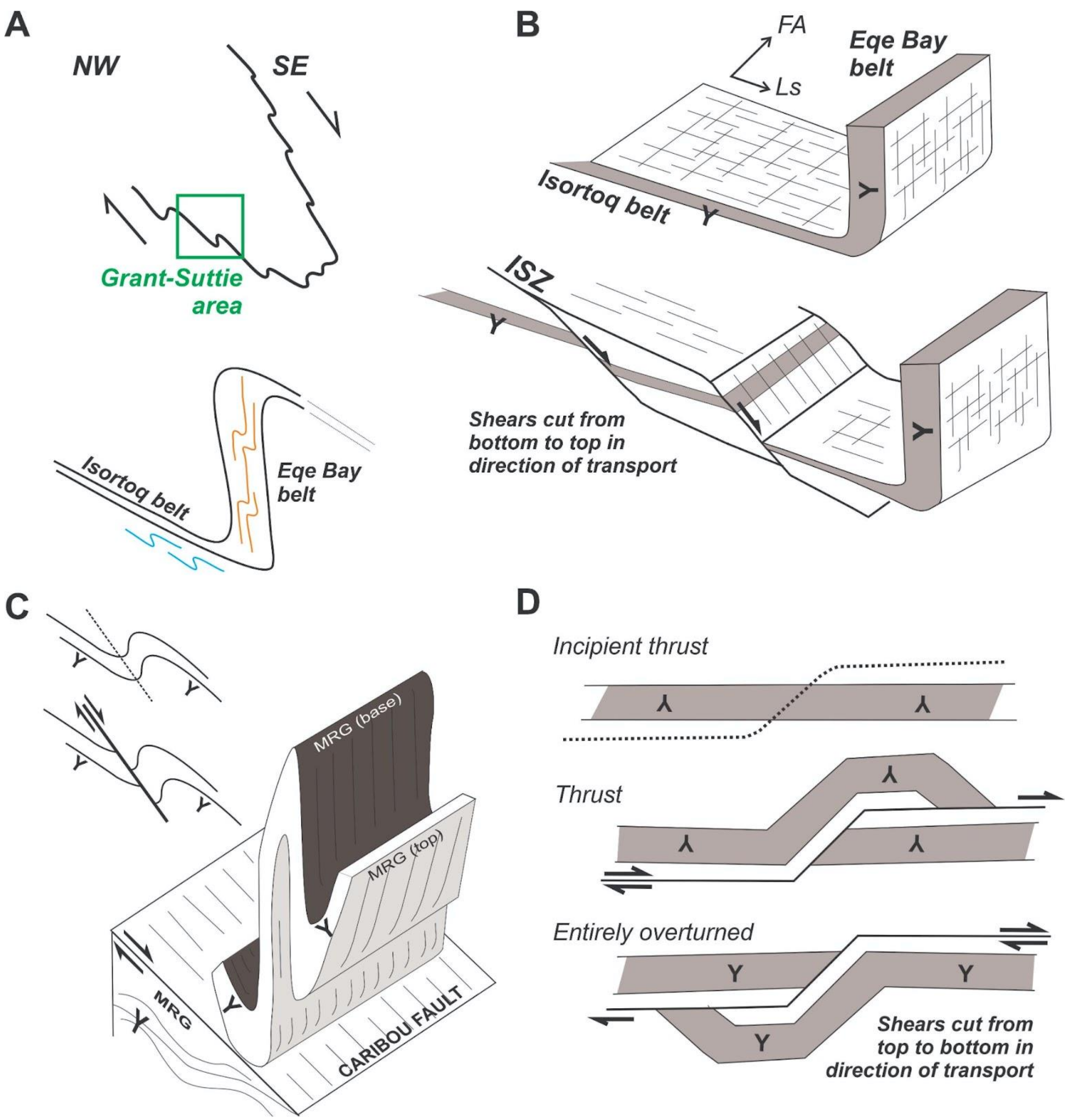
A
NW
SE
Grant-Suttie area
Isortoq belt
Eqe Bay belt
B
FA
Ls
Eqe Bay belt
Isortoq belt
ISZ
Shears cut from bottom to top in direction of transport
C
MRG (base)
MRG (top)
MRG
CARIBOU FAULT
D
Incipient thrust
Thrust
Entirely overturned
Shears cut from top to bottom in direction of transport

682 FIGURE 8

683

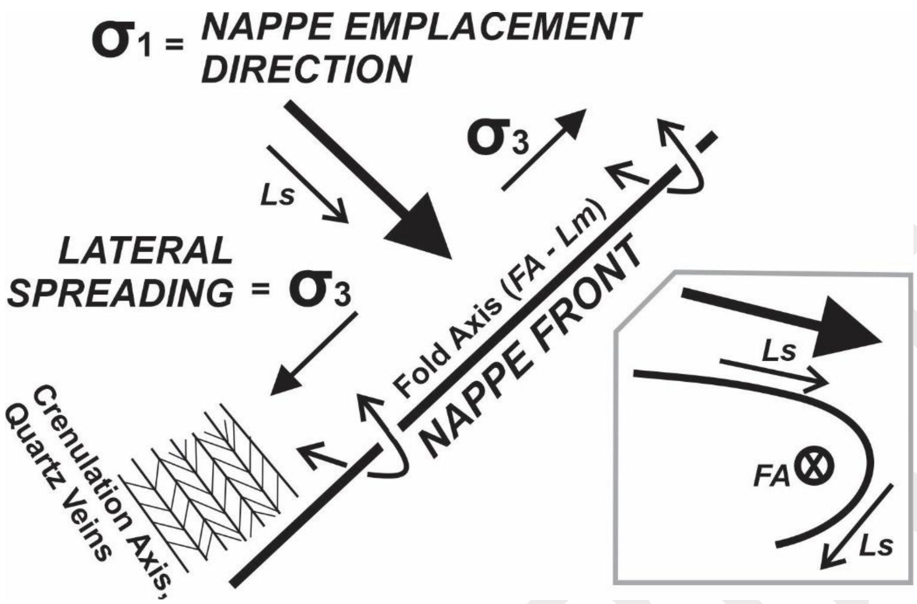

684

685